Theory of Energy Loss in Scanning Transmission Electron Microscopy of Supported Small Particles

A. Rivacoba,[1] N. Zabala,[2] and P. M. Echenique[1]

[1]*Departamento Fisica de Materiales, Facultad de Química, Universidad del Pais Vasco-Euskal Herriko Unibertsitatea, Apdo 1072, 20080 San Sebastian, Spain*

[2]*Departamento Electricidad y Electrónica, Facultad de Ciencias, Universidad del Pais Vasco-Euskal Herriko Unibertsitatea, Apdo 644, 48080 Bilbao, Spain*

(Received 9 April 1992)

A general expression for the energy loss probability in scanning transmission electron microscopy (STEM) is derived. The method uses a Green's function for the incident and scattered electrons and then folds the specimen into a local response function. Our expression is appropriate to any target geometry and dielectric response. As an application, the energy loss spectrum of a STEM electron moving close to an Al sphere half-embedded in an Al planar surface is calculated. The coupling between different l modes, neglected in earlier theoretical approaches, is taken into account.

PACS numbers: 71.45.Gm, 61.16.Di, 73.20.Mf, 79.20.Kz

The development of scanning transmission electron microscopy has stimulated and renewed the interest in the interaction of high-energy electron beams with surfaces and small particles [1–7]. In a typical STEM configuration, a well-focused 0.5-nm probe of 100-keV electrons provides a high-resolution transmission scanning image for samples with complex structures, such as catalyst or semiconductor devices. It also yields, from selected regions of the structure, x-ray emission spectra and electron energy loss spectra. Quantal theories [8–10] have been developed to analyze the experimental energy loss spectra in some simple cases.

Solutions, within the classical dielectric theory, have been worked out for a number of cases involving planar interfaces [11], spheres [12,13], cylinders [14–16], spheroids [17], and edges [18]. For these simple geometries, experimental results show that dielectric excitation theory is capable of predicting the loss spectra, allowing a fully consistent dielectric characterization of an interface or a small particle [19].

In many experimental situations the real problem is one of a mixed geometry, e.g., plane spherical, or two interpenetrating spheres [2,3,20–22]. Some authors have theoretically studied the surface modes of one sphere coupled to another surface (sphere [2,23] or plane [24]). In all those works the coupling among different multipolar terms was not taken into account, therefore their results are valid only for spheres at large distances or weakly coupled to the other surface. The theoretical approach by Wang and Cowley [20] to the problem of a half-embedded sphere mixes time and frequency in the derivation of the screened potential. Howie and Walsh [25] have presented results for the case of small Al particles in a matrix of AlF_3 and discussed them in terms of dielectric excitation theory for a two-phase medium. They showed that their data could not be interpreted in terms of any available effective medium theory [26–29]. A calculation for more complicated geometries could lay a foundation for the application of electron energy loss spectroscopy to a new range of challenging and important microstructural problems.

In this Letter we describe a general way of calculating results for spatially resolved electron energy loss spectroscopy. It does this by using a Green's function for the incident and scattered electrons and then folding the specimen structure into a local response function. Although we concentrate in this Letter on STEM, our method is general and, as we discuss in the conclusions, can be applied to other situations involving interaction of electrons with specimens of various geometries. Our approach decouples the probe from the specimen for calculation. This has not been generally accomplished in spatially resolved scattering. In addition it treats the probe as a wave packet from the start, thus exhibiting clearly the symmetry properties of the scattering. This is relevant and possibly important to STEM with probe sizes smaller than the lattice parameter, i.e., with the sub-Å probes the new 300-keV STEM is projected to have.

The probability $P(\omega)$ of losing energy ω, is related to the energy loss rate γ experienced by the particle, which in turn is given in terms of the imaginary part of the incident electron self-energy Σ_0, $\gamma = -2\mathrm{Im}(\Sigma_0)$ (we use atomic units throughout this paper).

The self-energy can be written in the pair approximation [30,31] in terms of the Green's function and the retarded screened interaction $W(\mathbf{r},\mathbf{r}',\omega)$. For STEM electrons the target is well described by a local dielectric function, the nonlocal effects are only relevant at very small distances between the probe and the surface ($\sim$Å) [32]. The averaged self-energy for the case of an electron interacting with the medium is then given by [9]

$$\Sigma_0 = \sum_f \int_0^\infty \frac{d\omega}{\pi} \int d\mathbf{r}\, d\mathbf{r}' \frac{[\Phi_0^*(\mathbf{r})\Phi_0(\mathbf{r}')\Phi_f^*(\mathbf{r}')\Phi_f(\mathbf{r})]}{\omega - E_0 + E_f - i\eta} \times \mathrm{Im}[W(\mathbf{r},\mathbf{r}',\omega)] , \quad (1)$$

where Φ_0, Φ_f, E_0, and E_f are the initial and final wave function and electron energies, and η is a positive infini-

tesimal. $W(\mathbf{r},\mathbf{r}',\omega)$ is the screened interaction, i.e., the solution of the Poisson equation for a unit charge at rest at $\mathbf{r}'$.

The incident electron wave packet Φ_0 is described

$$\Phi_0(\mathbf{r}) = \frac{1}{(2\pi)^2\sqrt{L}} \int d^2\mathbf{Q}\Phi_{\mathbf{Q}} e^{i\mathbf{Q}(\rho-\mathbf{b})} e^{i(k_0^2-Q^2)^{1/2}z}, \quad (2)$$

where k_0 is the incident electron momentum and $\Phi_{\mathbf{Q}}$ is chosen so that at $z=0$ the packet is distributed in a narrow probe about the impact parameter $\mathbf{b}$ with spatial extension Δ about $\mathbf{b}$. The factor in the wave function describing the z variation is normalized in the large spatial interval of length L.

To illustrate the application of the method we shall address the problem of energy loss of an electron interacting with a small spherical particle of radius a, half-embedded in a planar surface as shown in the scheme of the upper part of Fig. 1. A set of local dielectric functions $\varepsilon_i(\omega)$ $(i=1,3)$ (see Fig. 1) describe the three different media. The screened interaction in the external region can be written as follows:

$$W(\mathbf{r},\mathbf{r}',\omega) = \frac{2}{\varepsilon_1+\varepsilon_2} \sum_{L=0}^{\infty} \sum_{m=-L}^{L} \eta_{Lm} \frac{(L-m)!}{(L+m)!} \frac{r_<^L}{r_>^{L+1}} P_{Lm}(\mu) P_{Lm}(\mu') e^{im(\phi-\phi')} + \sum_{L=0}^{\infty} \sum_{m=-L}^{L} A_{Lm}(r',\mu') \frac{a^L}{r^{L+1}} P_{Lm}(\mu) e^{im(\phi-\phi')}, \quad (3)$$

where r, $\mu=\cos\theta$, and ϕ are the polar coordinates of $\mathbf{r}$ (or $\mathbf{r}'$ when stated). Here $\eta_{Lm}=1$ if $L+m$ is even or $\varepsilon_2/\varepsilon_1$ otherwise; $r_>$ and $r_<$ are, respectively, the largest and smallest of both r and r', and P_{Lm} are the Legendre functions. The first term on the right-hand side of Eq. (3) is the dynamical image solution corresponding to a planar interface [33], while the contribution of the sphere to the screened interaction is given by the second term. In the following we will concentrate on the energy loss due to the presence of the sphere, i.e., derived from the A_{Lm} terms; the η_{Lm} term gives rise to the well-known expression for the stopping power of a particle moving close to a plane [11]. From the matching conditions we obtain a system of linear equations (one for each value of m) in which all the multipoles are coupled

$$\frac{2}{\varepsilon_1+\varepsilon_2} \sum_L M_{Lj}^{(m)} \frac{(L-m)!}{(L+m)!} \{\eta_{Lm}[j\varepsilon_3 - L\varepsilon_1] + (-1)^{L+j}[j\varepsilon_3 - L\varepsilon_2]\} \left(\frac{a}{r'}\right)^{L+1} P_{Lm}(\mu') = -\sum_L M_{Lj}^{(m)} \left\{(L+1)\varepsilon_1 + j\varepsilon_3 + \frac{(-1)^{L+j}}{\eta_{Lm}}[(l+1)\varepsilon_2 + j\varepsilon_3]\right\} A_{Lm}, \quad (4)$$

where the matrix M is $M_{Lj}^m = \int_0^1 dx\, P_{Lm}(x) P_{jm}(x)$. The coupling among the multipoles implies that the collective modes of such a complex system are not related to a single multipolar term (as in the case of an isolated sphere). In general that system has to be solved numerically. 100 terms have been included in the following calculations.

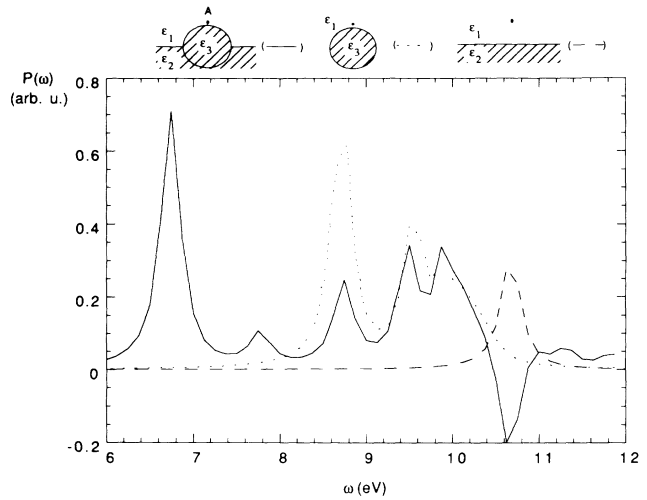

FIG. 1. Spectra corresponding to a 10-nm Al sphere half embedded in an Al surface (continuous line). The probe position into the plane (A) is shown above. The distance between the beam and the surface is 1 nm. Spectra corresponding to the same beam position near an isolated sphere (dotted line) and a planar interface of length $2a$ have been plotted (dashed line).

In the case of a well-focused beam along the z axis, with impact parameter $\mathbf{b}$, and parallel to the planar surface in which a target is lying, the probability of energy loss is given

$$P(\omega) = \frac{1}{\pi v^2} \int_{-\infty}^{\infty} dz \int_{-\infty}^{\infty} dz\, \mathrm{Im}[W(\mathbf{r},\mathbf{r}',\omega) e^{i(\omega/v)(z-z')}], \quad (5)$$

where the function $W(\mathbf{r},\mathbf{r}',\omega)$ is evaluated at $\rho=\rho'=\mathbf{b}$. Expression (4) is also valid for any target geometry.

We have computed the $P(\omega)$ for the case of a metallic sphere half embedded in an infinite medium of the same material. In Figs. 1 and 2 we show the spectra calculated for the case of a 100-keV electron beam in vacuum ($\varepsilon_1=1$), at grazing incidence close to the top (Fig. 1) and to the edge (Fig. 2) of a 10-nm Al sphere half embedded in an Al support. A Drude dielectric function with small damping has been used for Al ($\omega_p=15.1$ eV, $\gamma=0.27$ eV).

The spectrum of Fig. 1 is rather similar to that corresponding to an isolated sphere for values of ω above 9.5 eV. This similarity is due to the fact that for that partic-

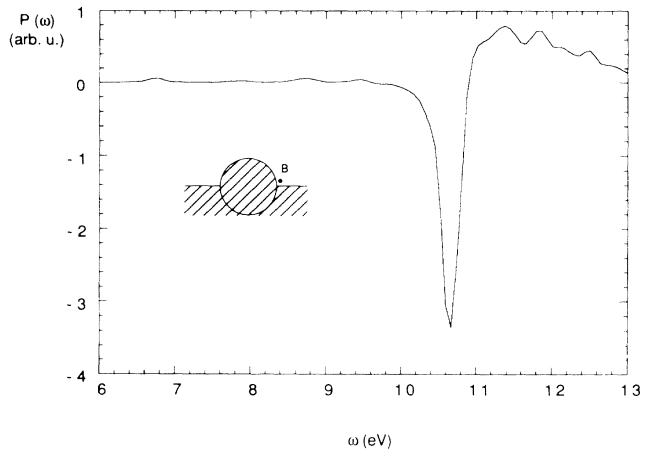

FIG. 2. Spectrum corresponding to a 10-nm Al sphere half embedded in an Al surface. The probe position into the plane (B) is shown above. The distance between the beam and both surfaces is 1 nm.

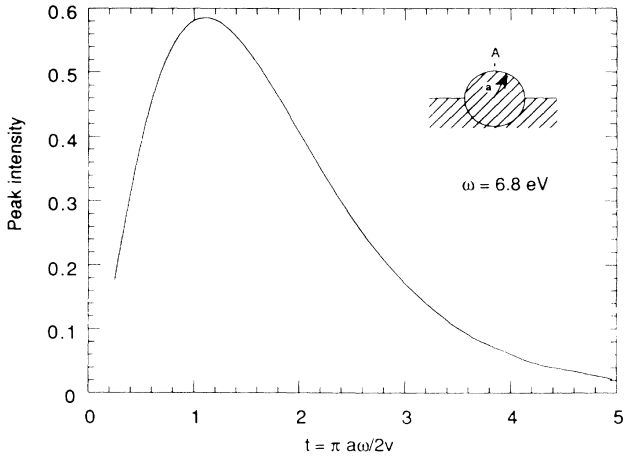

FIG. 3. Dependence of the height of the 6.8 eV with the reduced radius of the Al sphere half embedded in an Al support. The probe position is (A) as in Fig. 1. The distance between the beam and the surface has been kept constant (1 nm).

ular beam position the probe sees an almost spherical surface at the distances involved in those excitations (of the order of $v\omega^{-1}\sim 10$ nm in our case). Thus the support has little influence on such excitations. The main differences between both spectra are the existence of a new resonance at 6.8 eV, together with the lowering of the dipolar peak at 8.7 eV. The position of the 6.8 peak does not depend either on the size of the sphere or on the relative beam-target position (as it also happens with the modes of the single sphere). Thus this resonance is a new interface mode which appears due to the coupling between the plane and the sphere. This resonance does not take place in the case of an insulator support, therefore it can be attributed to the possibility of a new collective excitation originated by the grounding of the sphere by the infinite support. From the dependence of the peak intensity on the radius of the embedded sphere (Fig. 3) we conclude that this new mode is relevant only for spheres of radius smaller than 20–25 nm. The application of the method to the example points out a new observation—that some parts of the scattering are simple superposition of the constituent scattering while others are due only to the coupling among the constituents.

The more relevant part of the spectrum shown in Fig. 2 consists of some broad resonances above the planar surface plasmon at $\omega_s=\omega_p/\sqrt{2}$. This result is consistent with the modes of one edge [18]. Spectra of Figs. 1 and 2 correspond to extreme cases of the beam position; for any intermediate position of the beam all modes below and above ω_s take place in the spectrum.

In Figs. 1 and 2 the energy loss probability becomes negative in the neighborhood of 10.7 eV. This fact would be corrected by adding the contribution of the planar interface which has not been included in those spectra. It is well known that this spectrum (dashed line in Fig. 1) presents a peak centered on the planar surface plasmon, just where the negative values occur.

Experimental observations by Batson [2,3] on spherical targets have confirmed the existence of such a low-energy resonance as the main effect of the support. The particular scattering geometry of our example is different from that of the experiment of Batson and therefore it does not reproduce the dependence of the mode energy on relative sphere radii.

In conclusion, we have obtained a general expression for the energy loss probability of a STEM electron by using a Green's function for the incident and scattered electron and then folding the specimen structure into a local response function. Our formalism is relevant and possibly crucial to STEM with sub-Å probes. We have illustrated its use by evaluating the energy loss for the case of an electron beam interacting with a spherical particle half embedded in a planar support. We have established that the modes of such a complex system are those corresponding to the isolated sphere and the plane, plus some new resonances below and above the planar plasmon energy ω_s. Those new modes are associated with the coupling sphere/support. We estimate the size of the particles where this resonance can be relevant.

Our method is of more general interest than the application to STEM that we have discussed above. It can be of practical use in the study of optical properties of complex shapes and in problems involving electrons at surfaces such as the definition of an optical potential in low-energy electron diffraction and reflection high-energy electron diffraction [34,35] or in the interaction of electrons with surface states [36–40]. Of particular interest might be its application to STM: In this case a different Green's function should be used to describe the tunneling electron. The formalism could then serve to evaluate inelastic scattering and temperature increases in STM experiments.

The authors gratefully acknowledge Dr. C. M. M. Nex for his help and advice. The authors thank the Education Department of the Basque Country Government (project PGV9114.1), Guipuzkoako Foru Aldundia and Iberdrola for help and support and Labein for the use of computing facilities.

[1] P. E. Batson, Solid State Commun. **34**, 477 (1980).
[2] P. E. Batson, Phys. Rev. Lett. **49**, 936 (1982).
[3] P. E. Batson, Ultramicroscopy **9**, 277 (1982).
[4] A. Howie and R. H. Milne, J. Microscopy **136**, 279 (1984).
[5] A. Howie, Ultramicroscopy **11**, 141 (1983).
[6] A. Howie and C. A. Walsh, Radiat. Eff. Defects Solids **117**, 169 (1991).
[7] R. H. Ritchie, P. M. Echenique, F. Flores, and J. R. Manson, Radiat. Eff. Defects Solids **117**, 163 (1991).
[8] H. Kohl, Ultramicroscopy **11**, 53 (1983).
[9] P. M. Echenique, J. Bausells, and A. Rivacoba, Phys. Rev. B **35**, 1521 (1987).
[10] R. H. Ritchie and A. Howie, Philos. Mag. A **58**, 753 (1988).
[11] P. M. Echenique and J. B. Pendry, J. Phys. C **8**, 2936 (1975).
[12] T. L. Ferrell and P. M. Echenique, Phys. Rev. Lett. **55**, 1526 (1985).
[13] P. M. Echenique, A. Howie, and D. J. Wheatley, Philos. Mag. B **56**, 335 (1987).
[14] C. A. Walsh, Philos. Mag. **59**, 227 (1989).
[15] N. Zabala, A. Rivacoba, and P. M. Echenique, Surf. Sci. **209**, 465 (1989).
[16] C. A. Walsh, Ph.D. thesis, Cambridge, 1988 (unpublished).
[17] B. L. Illman, V. E. Anderson, R. J. Warmack, and T. L. Ferrell, Phys. Rev. B **38**, 3045 (1988).
[18] R. Garcia-Molina, A. Gras Marti, and R. H. Ritchie, Phys. Rev. B **31**, 121 (1985).
[19] M. G. Walls and A. Howie, Ultramicroscopy **28**, 40 (1989).
[20] Z. L. Wang and J. M. Cowley, Ultramicroscopy **21**, 77 (1987); **21**, 335 (1987); **21**, 347 (1987); **23**, 97 (1987).
[21] D. Ugarte, Doctor of Science thesis, University of Paris, 1990 (unpublished); D. Ugarte, C. Colliex, and P. Trebbia, Phys. Rev. B **45**, 4332 (1992).
[22] M. Schmeits and L. Dambly, Phys. Rev. B **44**, 12706 (1991).
[23] J. S. Nkoma, Surf. Sci. **245**, 207 (1991).
[24] N. Zabala and A. Rivacoba, Ultramicroscopy **35**, 145 (1991).
[25] A. Howie and C. A. Walsh, Microsc. Microanal. **2**, 171 (1991).
[26] J. C. Maxwell Garnett, Philos. Trans. R. Soc. **203**, 385 (1904).
[27] D. A. G. Bruggerman, Ann. Phys. (Leipzig) **24**, 636 (1985).
[28] D. Stroud and F. P. Pan, Phys. Rev. B **17**, 11602 (1978).
[29] A. Wachieski and M. C. McClung, Phys. Rev. B **33**, 8053 (1986).
[30] L. Hedin and S. Lundqvist, in *Solid State Physics,* edited by H. Ehrenreich and D. Turnbull (Academic, New York, 1969), Vol. 23, p. 1.
[31] J. R. Manson and R. H. Ritchie, Phys. Rev. B **24**, 4867 (1981).
[32] N. Zabala and P. M. Echenique, Ultramicroscopy **32**, 327 (1990).
[33] E. Zaremba, Surf. Sci. **151**, 91 (1985).
[34] J. B. Pendry, *Low Energy Electron Diffraction* (Academic, London, 1974).
[35] M. A. Van Hove and S. Y. Tong, *Surface Chrystallography by LEED* (Springer-Verlag, Berlin, 1979).
[36] J. P. R. Bolton and L. M. Brown, Proc. R. Soc. London A **428**, 291 (1990).
[37] S. V. Pepper, Surf. Sci. **123**, 47 (1982).
[38] P. M. Echenique and J. B. Pendry, J. Phys. C **11**, 2065 (1978).
[39] N. V. Smith, Phys. Rev. B **32**, 3549 (1985).
[40] P. M. Echenique and J. B. Pendry, Prog. Surf. Sci. **32**, 111 (1989).